

# 1 FORECASTING ALGAL BLOOM LAGS AND STABILITY IN A 2 WATERSHED\*

3 MACKENZIE JONES<sup>†</sup>, ALISON FRIDERES<sup>‡</sup>, BAILEY KRAMER<sup>§</sup>, AND FACULTY  
4 ADVISOR: KEITH WOJCIECHOWSKI<sup>§</sup>

5 **Abstract.** Near Menomonie, Wisconsin the lakes suffer from algae blooms during the warm  
6 summer months. Mathematical models describing the cyanobacteria population dynamics are studied  
7 with the intent of analyzing the conditions under which the populations grow and stabilize. Two  
8 models are considered, one for forecasting the population as the lake turns toxic from excess biomass  
9 after a flushing event occurs, and the other for establishing an algal bloom stability condition. These  
10 models are proposed for consideration to test the effectiveness of solutions put forth to ameliorate  
11 the algal bloom problem.

12 **Key words.** logistic growth, convection-diffusion, algal-bloom

13 **1. Introduction.** Eutrophication refers to the process of an ecosystem becoming  
14 more productive due to nutrient enrichment that stimulates primary producers [2].  
15 This process has led to the deterioration of lakes worldwide [5]. While eutrophication  
16 is thought to be part of the natural ontogeny of some lakes, it can be sped up through  
17 human activities [2]. Human driven eutrophication is a process that occurs rapidly  
18 and it can be difficult to reverse. It is caused mainly by point and non-point source  
19 inputs of nitrogen and phosphorus. These sources can be traced largely to agricultural  
20 practices, deforestation, and the release of sewage into the watershed. The resulting  
21 change in water chemistry leads to a shift in species composition where phytoplankton  
22 dominate macrophytes [2]. These changes often lead to decreased water quality and  
23 increased algal blooms.

24 Algal blooms cause unwanted outcomes in impacted watersheds. Thick blooms  
25 around the edges of a lake can prevent people from swimming and taking watercraft  
26 out onto the lake. A degraded lake causes surrounding houses to be priced lower and  
27 area tourism to decrease [1, 8]. Additionally, these blooms can produce liver toxins  
28 that are potentially deadly to wildlife utilizing the lake, including humans [9]. One of  
29 the main producers of toxic algal blooms is the cyanobacteria *Microcystis aeruginosa*, a  
30 bacterium that lives in eutrophic freshwater. *M. aeruginosa* are not greatly impacted  
31 by competition or predators. Cyanobacteria are able to outcompete other species  
32 for light by employing chlorophylls, carotenoids, and phycobilins that allow them to  
33 obtain light energy from areas of the spectrum that other taxa cannot utilize [10]. The  
34 optimal growth temperature of cyanobacteria is much higher than other eukaryotic  
35 taxa and cyanobacterial blooms have been associated with an increase in local water  
36 temperatures. This means that cyanobacteria are able to bring their surrounding  
37 environment to a temperature that is both better for their own optimal growth and  
38 detrimental to the growth of their competitors. Furthermore, *M. aeruginosa* are able  
39 to utilize gas vesicles which can be manipulated to change size and density in order to  
40 regulate buoyancy. These gas vesicles, along with a resistance to ultraviolet radiation,  
41 allow the cyanobacteria to shade out non-buoyant phytoplankton and macrophytes

---

\*Submitted to the editors DATE.

**Funding:** This work was funded by the National Science Foundation SMA grant no. 135738.

<sup>†</sup>Department of Mathematics, University of Akron, Akron, OH ([mlj54@zips.uakron.edu](mailto:mlj54@zips.uakron.edu)).

<sup>‡</sup>Department of Mathematics, Simpson College, Indianola, IA ([allison.frideres@my.simpson.edu](mailto:allison.frideres@my.simpson.edu)).

<sup>§</sup>Department of Mathematics, Statistics, and Computer Science, University of Wisconsin Stout, Menomonie, WI ([kramerb0587@my.uwstout.edu](mailto:kramerb0587@my.uwstout.edu), [wojciechowskik@uwstout.edu](mailto:wojciechowskik@uwstout.edu)).

42 [10].

43 There is evidence that *M. aeruginosa* are able to use multiple different methods  
44 to avoid predation. Many strains can produce cyanotoxins, which are broad spectrum  
45 and make the cyanobacteria difficult to consume. *M. aeruginosa* are also covered in  
46 a gelatinous coating. There is evidence that this makes them indigestible to many  
47 species and there is further evidence that some strains are still viable after passing  
48 through the gut of grazers. Moreover, the cyanobacteria accumulate in overwhelming  
49 numbers. At such high densities it is possible that the negative impact any grazers may  
50 have on the cyanobacteria population is outweighed by the size of that population.  
51 Furthermore, while there exist bacteria viruses in the lake that cause cyanobacteria  
52 death, the numbers are not sufficient to greatly affect the large cyanobacteria pop-  
53 ulation [9]. The large size and density of the cyanobacteria population also reduces  
54 the ability of grazers to reach and consume other prey which ultimately decreases the  
55 fitness of the grazer.

56 These adaptations decrease pressures from predation and competition causing  
57 cyanobacteria to be more limited by environmental factors such as a need for sunlight,  
58 an optimum growth temperature, a high nitrogen to phosphorus ratio, low turbulence,  
59 and a long residence time. Cyanobacteria may favor strong sun exposure because they  
60 excel in waters that periodically exceed 20 degrees Celsius, with surface forming genera  
61 reaching optimal temperatures around 25 degrees Celsius. *M. aeruginosa* is a non-N<sub>2</sub>  
62 fixing species, meaning it cannot transform inorganic forms of nitrogen into a viable  
63 form for photosynthesis [10]. In order for cyanobacteria to grow and produce organic  
64 matter there must be a large amount of nitrogen freely available to them.

65 Low turbidity, long residence times, and calm surface waters are also needed for  
66 optimal growth [10]. In order to uptake nutrients, the cyanobacteria utilize their gas  
67 vesicles to sink to the bottom of the lake and then float back up to the surface to  
68 get necessary sunlight. If a lake is highly turbulent, it becomes more difficult for  
69 *M. aeruginosa* to maintain an optimal vertical position, allowing non-motile species  
70 to have a greater competitive advantage. Cyanobacteria are able to consume more  
71 phosphorus than necessary for biological production and store it for later use, as well  
72 as sequester essential trace nutrients like iron [7, 10]. Long residence times, without  
73 flushing the lake, allow cyanobacteria to uptake high amounts of phosphorus and  
74 produce blooms before a high turbulence event occurs. High flow events followed  
75 by periods of long residence time can be beneficial to cyanobacteria as the inflow  
76 often brings more nutrients into the lake [10]. If growth conditions are met, it takes  
77 approximately 5-7 days for the cyanobacteria to double in population [9].

78 These ideal growth conditions occur seasonally in Tainter Lake, a 1605 acre eu-  
79 trophic reservoir in Dunn County, Wisconsin [18]. The Red Cedar and Hay Rivers  
80 inflow into the lake which was created by damming the Red Cedar River downstream.  
81 Tainter Lake outflows into the Red Cedar River toward Lake Menomin, a lake with  
82 a similar bloom situation. In general, blooms tend to be more severe in late summer,  
83 when there is often less rainfall and warmer temperatures. In Tainter Lake the phos-  
84 phorus levels are deemed eutrophic based on the trophic status index. These high  
85 levels are caused from phosphorus in the sediment, agricultural runoff, and inputs  
86 from several other eutrophic lakes in the watershed [16].

87 The Tainter Lake reservoir has a maximum depth of approximately 11.3 meters  
88 and an average depth of about 4.3 meters [18]. Unlike many previously studied lakes  
89 with similar bloom conditions, Tainter Lake has a general lack of stratification with  
90 regards to water temperature, since stratification primarily occurs in deeper lakes  
91 when there is seasonal turnover. Figure 1 shows temperature stratification based

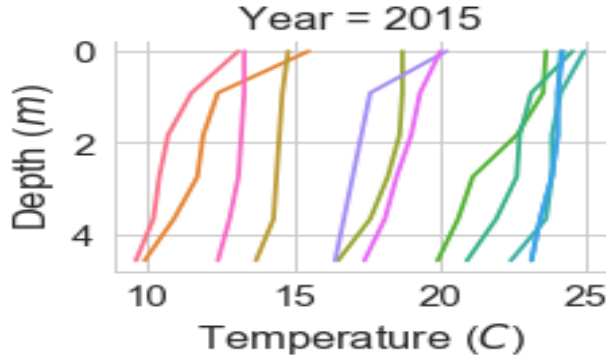


FIG. 1. Temperature stratification based on depth of Tainter Lake with different colors representing data collected on different days

92 on depth of Tainter Lake in the year 2015. The different colors represent different  
 93 days the temperature measurements were taken, from April to October. Warmest  
 94 temperatures occur from June to August and are represented by the green and blue  
 95 lines. The coldest temperatures occur in April to May and September to October and  
 96 are represented by the pink and orange lines. All lines are mostly vertical meaning  
 97 there is no thermocline or temperature differences at different depths of the lake.

98 A search of the literature reveals that existing models have not been calibrated  
 99 to conditions similar to those found in Tainter Lake. Therefore a modified model is  
 100 needed in order to test proposed mitigation measures to cyanobacterial dominance in  
 101 lakes with these conditions. The modified model could then be run with the proposed  
 102 parameters to see if there would be any decrease in the cyanobacteria population.

103 Two models are proposed. The first is an initial value problem (IVP) containing  
 104 an ordinary differential equation. This IVP is a modified logistic model for forecasting  
 105 the chlorophyll-a concentration after flushing event has occurred and the lake has  
 106 resumed calm surface waters to precipitate optimal growth. The advantage of this  
 107 model is that it is simple to understand the simulation results and more simulations  
 108 can be run with this model. The disadvantage of this model is that it can only predict  
 109 chlorophyll concentration over shorter time spans of one month.

110 This model was motivated to understand the short-term growth patterns of algae.  
 111 After a rainstorm, most algae are flushed out of the lake and phosphorus runoff is  
 112 channeled into the lake. The low population of algae takes approximately 5 days to  
 113 double its population and several weeks to reach a saturation concentration. Since  
 114 there is a lag time for the algae to uptake the phosphorus nutrients and grow, it does  
 115 not automatically seem apparent that excess phosphorus leads to algae growth. This  
 116 model was created to dispel the misunderstanding that phosphorus does not cause  
 117 algae growth.

118 The second is an initial boundary value problem (IBVP) containing a partial  
 119 differential equation. This IBVP is a convection diffusion equation with a source  
 120 term used to construct a bloom stability condition solely dependent upon the sinking  
 121 velocity of the bacteria and the euphotic layer. If lake conditions cause this condition  
 122 to fall below a certain threshold, then the *M. aeruginosa* population will collapse.  
 123 The advantage to this model is that it helps us understand the biologic and limnologic  
 124 conditions that lead to algae blooms. The disadvantage is that it is more difficult to

125 understand and run numerical experiments with.

126 This model was motivated to understand the longer-term growth patterns of algae.  
 127 Instead of examining chlorophyll-a concentration over time, this model is used for  
 128 predicting whether the lake conditions are conducive for an algae bloom. This model  
 129 gives us solutions to bring about population collapse by varying the turbulence of the  
 130 water or by manipulating the algae growth rate.

131 This paper is organized as follows. Section 2.2 contains a description of Tainter  
 132 Lake and examines the IVP used to forecast the chlorophyll-a concentration. The  
 133 IVP is solved analytically as well as numerically to generate an envelope of solutions  
 134 dependent upon a variety of input parameters. Section 3 analyzes the IBVP used to  
 135 model the chlorophyll-a concentration as function of time and depth. The IBVP is  
 136 nondimensionalized and analytically solved to arrive at a threshold for the sinking  
 137 velocity and euphotic layer.

138 This paper contributes to the literature by modifying current models to fit the  
 139 unique limnologic conditions of Tainter Lake, being a shallower lake with no thermo-  
 140 cline. In addition, we provide two models with different ways of thinking about the  
 141 problem from a short term and longer term perspective. Two models were needed  
 142 because the first provides understanding of how algae uptake phosphorus to grow and  
 143 take several weeks to reach a bloom level. The next model was necessary to discover  
 144 the biologic and limnologic conditions that will bring about a population collapse. Both  
 145 models can be used as public policy tools to understand the various options to solve  
 146 the algal bloom problem.

## 147 2. Chlorophyll Forecast.

148 **2.1. Lake Conditions.** The model used to forecast the chlorophyll-a concen-  
 149 tration is primarily informed by field observations obtained by James et. al. through  
 150 a research experience for undergraduates (REU) and the Wisconsin Department of  
 151 Natural Resources (DNR) [4, 17]. Weather data, such as rainfall, was collected by  
 152 Weather Underground at Colfax, WI, about 8 kilometers from Tainter Lake [15].  
 153 Daily flow data was retrieved from the United States Geographical Survey (USGS)  
 154 [14].

155 The summer of 2015 was not considered a drought year, receiving regular rainfall  
 156 that allowed for minor to major flushing. Thus, the blooms experienced were generally  
 157 not as severe as in previous years. For the scope of this paper, a chlorophyll-a mea-  
 158 surement greater than or equal to  $40 \mu\text{g/L}$  is considered a bloom event. The weather  
 159 and flow conditions, as well as the occurrence of bloom conditions in the chlorophyll  
 160 data, are shown in Figure 2. Here, the purple squares represent bloom events and  
 161 the green circles represent non-bloom events. Blooms generally occurred in periods of  
 162 warmer weather and lower flow. Figures 1 and 2 are used to illustrate the conditions  
 163 of Tainter Lake. While these data are not used in verifying either model proposed  
 164 they are used in justifying why new models are proposed. The conditions of Tainter  
 165 Lake differ from other lakes studied so new models and calibrations were needed.

166 One significant flushing event occurred in early July of 2015, as seen in Figure 3.  
 167 Bloom events were not recorded for several weeks following the flushing event. A ma-  
 168 jor bloom event, the highest in the recorded data at a CHL-a level of  $197.38 \mu\text{g/L}$ , was  
 169 recorded approximately three weeks after the flushing occurred. This lag indicates  
 170 that a spike in rainfall flushes the chlorophyll-a from the lake and the *M. aeruginosa*  
 171 subsequently recovers. The population consumes the latent and newly introduced re-  
 172 sources to grow over this period before it reaches an equilibrium. A modified logistic  
 173 model can capture this behavior and is used to forecast the chlorophyll-a concentra-

FORECASTING ALGAL BLOOM LAGS AND STABILITY

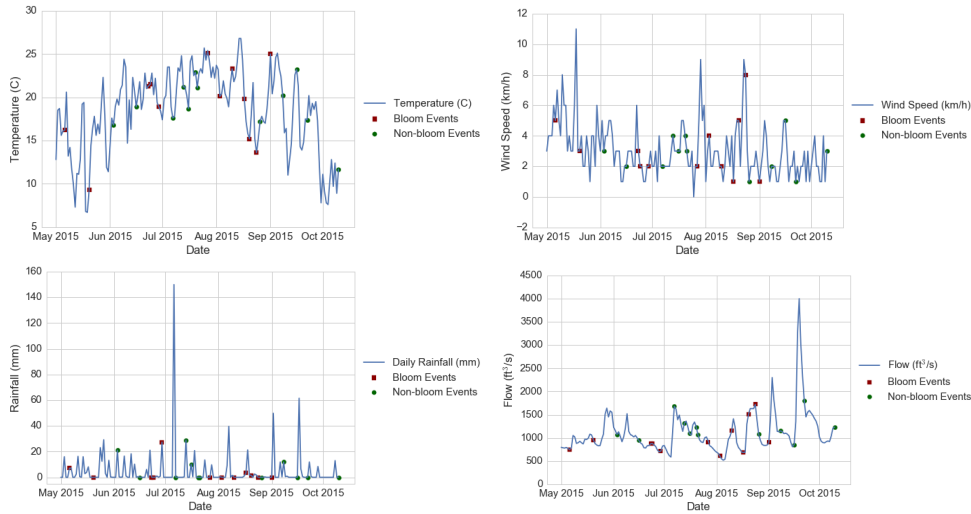


FIG. 2. May 1 - October 10, 2015: Daily temperature (C), wind speed (km/h), rainfall (mm), and flow readings (ft<sup>2</sup>/s)

174 tion. This data is used to verify model (2.1).

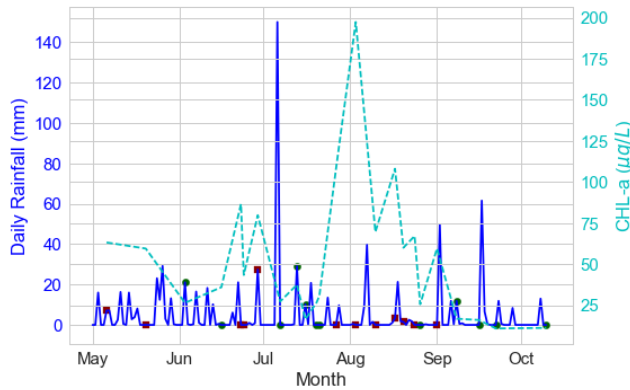


FIG. 3. May 1 - October 10, 2015: Daily rainfall (mm) and CHL-a (µg/L) trends in Tainter Lake.

175 There is no standard chlorophyll-a measurement that denotes a bloom, the only  
 176 requirement is a rapid increase in algal population. Since 40 µg/L is enough to cause  
 177 discoloration of the water and classifies the lake as eutrophic, this estimate is used for  
 178 a bloom level event. The result that a bloom occurs 3 weeks after a flushing event  
 179 is robust to changes in this definition of an algae bloom. Our results are consistent  
 180 for any threshold level chosen between 30 to 110 µg/L. If a level under 30 µg/L is  
 181 chosen as the threshold value then it only takes 1 week for the algae population to  
 182 reach bloom levels after a flushing event. If a level over 110 µg/L is chosen as the  
 183 threshold value then it takes 4 weeks for the algae population to reach bloom levels.  
 184 Regardless of the threshold value chosen, the results display the behavior that there  
 185 is a time lag between the rainfall event and an algal bloom. In addition, as will be

186 shown in Section 2.2, higher growth rates will cause the algae population to reach the  
 187 steady state more quickly.

188 **2.2. Forecast Model.** A logistic growth model was adapted from [13] in order  
 189 to simply and accurately forecast chlorophyll levels. The equation provided in  
 190 [13] predicts chlorophyll concentration under nutrient-limited circumstances in an im-  
 191 poundment over a period of a few days. However, the exponential model is realistic  
 192 for short-term growth and since it was desirable to forecast chlorophyll levels over a  
 193 monthly period a carrying capacity term was added to place a bound on the concen-  
 194 tration. A longer period was required to predict concentration levels when a flushing  
 195 event might not occur within 21 days. Such periods might be the result of a drought  
 196 or simply low rainfall levels during the summer. During such periods the lake be-  
 197 comes noisome and residents report conditions surrounding the lake are intolerable.  
 198 These so-called “saturation periods” may be cause of low property values for homes  
 199 surrounding the lake [11].

200 The proposed logistic model, written as an initial value problem (IVP) is,

201 (2.1) 
$$\begin{cases} \frac{dC}{dt} = C_i F + (\mu - F) \left(1 - \frac{C}{K}\right) C \\ C(0) = C_0 \end{cases}$$

202 where  $C$  is the chlorophyll concentration at any point of the lake,  $K$  is a saturation  
 203 parameter,  $C_i$  is the concentration of chlorophyll at the inflow of the lake,  $F$  is the  
 204 flushing rate, and  $C_0$  is the initial concentration.

Parameter	Description	Value	Units	Source
<i>Chlorophyll Forecast</i>				
$C(0)$	Initial chlorophyll	10	$\mu\text{gL}^{-1}$	James [4]
$C_i$	Inflow chlorophyll	10	$\mu\text{gL}^{-1}$	James [4]
$\mu$	Chlorophyll growth rate	0.30	$d^{-1}$	Søballe [13]
$F$	Flushing rate	0.13	$d^{-1}$	DNR [16]
$C_\infty$	Steady state chlorophyll	$175 \pm 29$	$\mu\text{gL}^{-1}$	DNR [16]
$K$	Steady state parameter	167.7	$\mu\text{gL}^{-1}$	Simulations

205  
 206  
 207  
 208 The solution to IVP (2.1) is,

209 
$$C(t) = C_\infty^+ \frac{1 - \frac{C_\infty^-}{C_\infty^+} \left(\frac{C_0 - C_\infty^+}{C_0 - C_\infty^-}\right) e^{-\sqrt{(\mu-F)^2 + 4C_i F \frac{\mu-F}{K}} t}}{1 - \left(\frac{C_0 - C_\infty^+}{C_0 - C_\infty^-}\right) e^{-\sqrt{(\mu-F)^2 + 4C_i F \frac{\mu-F}{K}} t}},$$

210 where,  $C_\infty^-$  and  $C_\infty^+$  are given by,

211 (2.2) 
$$C_\infty^\pm = \frac{K}{2} \left( 1 \pm \sqrt{1 + 4 \frac{C_i F}{\mu - F}} \right).$$

212 The steady-state solution is  $\lim_{t \rightarrow \infty} C(t) = C_\infty^+$ . For this paper, we assume  $\mu > F$ ,  
 213 which is reasonable for our data set because  $\mu > 2F$ . If  $\mu < F$ , then physically  
 214 this scenario corresponds to flushing the chlorophyll from the lake. This case is  
 215 mathematically interesting but outside the regime of applicability for the physical  
 216 case so we neglect it when running simulations.

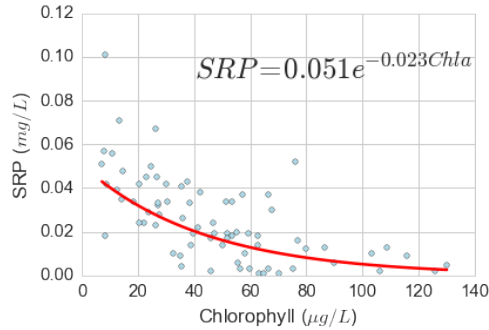


FIG. 4. 2015 REU data to examine the relationship between CHL-a and SRP to get an estimate for chlorophyll saturation level.

217 The flushing rate and growth rate were estimated from DNR data and similar  
 218 values were also confirmed in [13]. To estimate  $C_{\infty}^{+}$ , previous field and laboratory  
 219 observations obtained by an REU and the DNR were analyzed to get an estimate  
 220 [4, 17]. Figure 4 shows a plot of chlorophyll concentration against soluble reactive  
 221 phosphorus. This data, collected by the REU, was analyzed to get an estimation  
 222 of the saturation point under nutrient limited conditions, then this estimate was  
 223 checked against previous years of DNR data. An estimate of 140  $\mu\text{g/L}$  of chlorophyll  
 224 was observed from the REU data and a maximum value of 200  $\mu\text{g/L}$  was found in the  
 225 DNR data. To reconcile the difference, an estimate of 175  $\mu\text{g/L}$  was used. The results  
 226 are robust to changes in the steady state value. For a given  $\mu$ , it takes approximately  
 227 3 weeks to reach the steady state for any saturation level between 130 to 250  $\mu\text{g/L}$ .

228 A carrying capacity was estimated using the previous value for  $C_{\infty}^{+}$  in equation  
 229 (2.2) to get a value of 175  $\mu\text{g/L}$ . The standard deviation was determined by looking  
 230 at DNR data [16] to get a value of 29  $\mu\text{g/L}$ . To run the first set of simulations, all  
 231 parameters were held fixed except for the saturation value which was assumed to be  
 232 normally distributed around mean 175  $\mu\text{g/L}$  with standard deviation 29  $\mu\text{g/L}$ . In  
 233 addition, a flushing rate of  $.13 \text{ d}^{-1}$  and a growth rate of  $.3 \text{ d}^{-1}$  were used, as obtained  
 234 from DNR data [16]. The simulation was run using 100 realizations over a simulation  
 235 time of 4 weeks. The realizations are indicated by the black lines and the average  
 236 growth profile was computed and is indicated by the white dashed curve in Figure 5.  
 237 IVP (2.1) was solved numerically using lsoda from the FORTRAN library odepack  
 238 embedded within Scipy [12].

239 This model assumes an initial condition immediately after a large flushing event  
 240 when the chlorophyll concentration is low, set to  $10 \mu\text{g/L}$ , and predicts what will  
 241 happen if there is not another large rain event to flush the chlorophyll out of the lake.  
 242 Under these conditions, the model shows that with average growth the population  
 243 will hit a saturation level in approximately 3 weeks as shown in Figure 5. This result  
 244 corresponds well with what is found in the DNR data that after a flushing event the  
 245 chlorophyll levels take about 3 weeks to hit saturation levels because the doubling  
 246 time for *M. aeruginosa* is approximately 3-5 days and there is a lag time for them to  
 247 gather nutrients before starting to rapidly grow. This model confirms the fact that  
 248 there is a lag time for algae growth after a flushing event.

249 A second set of simulations were also run with varying growth rate,  $\mu = 0.3 \pm$   
 250  $0.1 \text{ d}^{-1}$ . The other parameters are held fixed with a flushing rate a flushing rate of  $.13$   
 251  $\text{d}^{-1}$  and a saturation level of 175  $\mu\text{g/L}$ . The results are shown in Figure 6. This figure

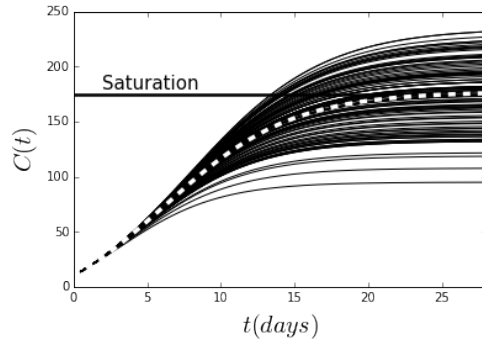


FIG. 5. *Envelope of solutions after 100 realizations with varying steady-state solution  $C_{\infty}^+ = 175 \pm 29 \mu \text{ g/L}$ . The horizontal line indicates chlorophyll saturation and the thick dotted line indicates average concentration growth.*

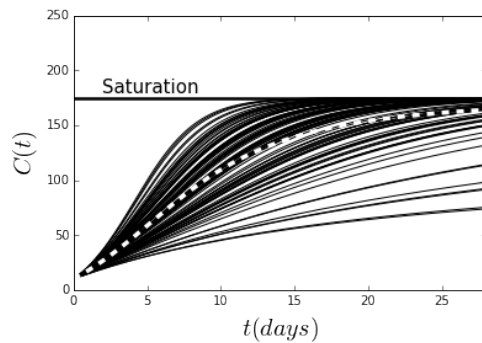


FIG. 6. *Envelope of solutions after 100 realizations with varying growth parameter,  $\mu = 0.3 \pm 0.1 \text{ d}^{-1}$ . The horizontal line indicates chlorophyll saturation and the thick dotted line indicates average concentration growth.*

252 also shows that the population takes approximately 3 weeks to hit saturation level.  
 253 However, in Figure 5 solutions could end up less than or greater than the saturation  
 254 level, while in Figure 6 all solutions are bounded by the saturation level.

255 To account for variation in the data and to test the sensitivity of the results,  
 256 additional simulations are run with other growth parameter values. Figure 7 shows  
 257 simulations being run with the growth parameter between  $0.2$  to  $0.7 \text{ d}^{-1}$  with the same  
 258 standard deviation of  $0.1 \text{ d}^{-1}$ . With higher growth rates the sample growth profiles  
 259 converge more quickly to the average growth profile. In addition, as  $\mu$  increases the  
 260 saturation level is reached more quickly. It takes the average growth profile about 20  
 261 to 25 days to reach saturation when  $\mu = 0.3$  and it takes about 10 days when  $\mu =$   
 262  $0.8$ . This is intuitive because when algae grow at a faster rate they should reach the  
 263 saturation level more quickly.

### 264 3. Bloom Stability.

265 **3.1. Bloom Model.** Simulating cyanobacteria growth was done by using a  
 266 parabolic partial differential equation modified from Johnk's phytoplankton competi-  
 267 tion model [6]. Cyanobacteria are only considered in this model because little compe-  
 268 tition exists from other phytoplankton species that influence cyanobacterial growth;



FORECASTING ALGAL BLOOM LAGS AND STABILITY

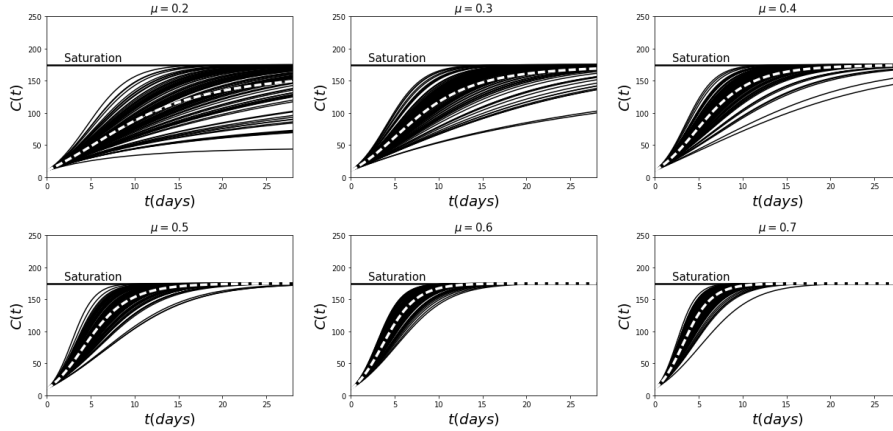


FIG. 7. *Envelope of solutions after 100 realizations with varying growth parameters. The horizontal line indicates chlorophyll saturation and the thick dotted line indicates average concentration growth.*

269 these other species are also not bothersome or toxic to Tainter Lake. It should be  
 270 noted that this model is not used to predict cyanobacteria concentration at a certain  
 271 time but it will be used to predict whether the given lake conditions are viable for an  
 272 algae bloom to occur. This model is separate from model (2.1) and provides different  
 273 solutions to solve the problem.

274 The chlorophyll concentration is modeled here since there was only available data  
 275 on amount of chlorophyll in the lake. Cyanobacteria population can be backed out of  
 276 the model since there is a strong positively linear relationship between chlorophyll and  
 277 population. Due to this relationship, linear regression equations have been modeled  
 278 so once the chlorophyll level is known the population can be estimated from the  
 279 regression equation.

280 Chlorophyll is a byproduct of algal growth which is influenced by phosphorus, light  
 281 availability, temperature, and turbulence. The chlorophyll concentration dynamic is  
 282 described by:

$$\begin{cases} \frac{\partial C}{\partial t} = \mu(I, T)C - m(T)C + \frac{\partial}{\partial z}(v(T)C) + \frac{\partial}{\partial z}(D_z \frac{\partial C}{\partial z}) \\ l v_{surface} C(0, t) - D_z \frac{\partial C}{\partial z} = 0 \\ C(1, t) = 0 \\ C(z, 0) = f(z) \end{cases}$$

283 (3.1)

284 Where  $C(z, t)$  denotes the chlorophyll concentration ( $\mu\text{g/L}$ ) at time  $t$  (s) and depth  
 285  $z$  (m) with  $l$  being the bottom depth,  $I(z, t)$  ( $\mu\text{mol/m}^2\text{s}$ ) denotes the intensity of  
 286 the light that is available for photosynthesis and  $T(z, t)$  denotes the temperature in  
 287 Celsius. Temperature was gathered from previous DNR data and irradiance will be  
 288 calculated as it depends on the amount of chlorophyll in the water, since more chloro-  
 289 phyll indicates murkier waters. Further,  $\mu(I, T)$  represents the specific growth rate  
 290 and is dependent upon the amount of light, temperature and heat that the cyanobac-  
 291 teria receives; conversely,  $m(T)$  represents the mortality rate which is assumed to  
 292 be solely dependent on temperature. The term  $v(T)$  (m/s) is the vertical velocity  
 293 and since cyanobacteria have gas vacuoles that make them float their vertical float

294 velocity and the chlorophyll that floats with them will be positive. The magnitude of  
 295 the velocity is dependent upon the dynamic viscosity of water which is dependent on  
 296 temperature. Lastly,  $D_z$  is the vertical turbulent diffusivity which can be obtained  
 297 from DNR data on the momentum and temperature of the water. A zero-mass flux  
 298 continuity boundary condition is imposed at the surface of the lake since chlorophyll  
 299 cannot leave or enter the lake and the concentration of chlorophyll stays continuous  
 300 throughout the depth of the lake. A zero concentration boundary condition is im-  
 301 posed at the bottom of the lake. We assume no chlorophyll exists at the bottom of  
 302 the lake which is reasonable because light does not reach the bottom of the lake for  
 303 cyanobacteria to thrive and produce chlorophyll. Several initial conditions were used  
 304 and did not have a large impact on the results.

305 The underwater light intensity may change due to increased chlorophyll because of  
 306 a larger number of cyanobacteria. This relationship can be described with a Lambert-  
 307 Beer's law:

308 
$$I(z, t) = I_{in}(t)(1 - r) \exp \left( - \int_0^z \kappa C(\sigma, t) d\sigma - K_{bg} z \right).$$

309 Where  $I_{in}(t)$  is the incident light intensity that can be used for photosynthesis  
 310 at the surface. Wave reflectivity is represented as  $r$ , implying  $(1 - r)$  corrects for any  
 311 reflection losses at the surface. The light attenuation coefficient for cyanobacteria,  
 312  $\kappa$ , represents how easily light can be penetrated due to the cyanobacteria biomass.  
 313 The background attenuation coefficient,  $K_{bg}$ , represents how easily the water can  
 314 be penetrated by light due to non-phytoplankton, and  $\sigma$  is a dummy integration  
 315 variable accounting for the non-constant cyanobacteria distribution in depth. To find  
 316 the initial irradiance  $I_{in}(t)$ , the following relation is used:

317 
$$I_{in} = (1 - 0.65C_l^2)I_{sol},$$

318 where  $C_l$  represents the amount of cloud cover ( $0 < C_l < 1$ ) and  $I_{sol}$  is the amount  
 319 of solar radiation for a sky without cloud cover.

320 The growth rate due to irradiance is described by a Monod equation, which  
 321 relates microorganism growth rate to the concentration of a limiting nutrient in the  
 322 environment. Irradiance is focused on as the limiting nutrient because Tainter Lake is  
 323 highly eutrophic and the cyanobacteria can get all of the phosphorus that they need to  
 324 grow. However, their phosphorus uptake rate does have some impact on their growth  
 325 rate which then impacts the lake's bloom rate, which will be taken into account in  
 326 future work. The relationship between growth rate and light intensity is described  
 327 using a Monod model:

328 
$$\mu(I, T) = \frac{\mu_{\max}(T)I}{\mu_{\max}(T)/\alpha + I},$$

329 where  $\mu_{\max}(T)$  is the maximum growth rate at the light-saturation point as a  
 330 function of temperature, which is where increases in light intensity do not increase  
 331 the photosynthetic rate; and  $\alpha$  is the initial slope of the growth curve under light-  
 332 limited conditions. The maximum growth rate is determined from the dark reaction  
 333 of photosynthesis, which does not need light to occur, and because of the enzymes  
 334 used it is temperature dependent. The slope  $\alpha$  is determined from the light reaction  
 335 of photosynthesis which is dependent on light intensity and absorption but not on  
 336 temperature.

337 The maximum growth rate is modeled by an Arrhenius relationship which de-  
 338 scribes the temperature dependence on growth rates. The growth rate increases with

339 increases in temperature until an optimum temperature,  $T_{opt}$ , is reached and then the  
 340 growth rate decreases. The maximum growth rate is modeled as:

$$341 \quad \mu_{max}(T) = \mu_{max}(T_{opt}) \left[ 1 + b \left( \left( R_1^{T-T_{opt}} - 1 \right) - \frac{\ln(R_1)}{\ln(R_2)} \left( R_2^{T-T_{opt}} - 1 \right) \right) \right],$$

342 where  $\mu_{max}(T_{opt})$  is the maximum growth rate at the optimum temperature,  
 343 and  $R_1, R_2$ , and  $b$  describe the shape of the optimum curve. The mortality rate is  
 344 dependent on temperature and is assumed to grow exponentially. This assumption  
 345 is made since growth rate increases with temperature however when there are more  
 346 bacteria there is more competition for nutrients and the environment cannot sustain as  
 347 many new cyanobacteria so, more must die in order to keep balance. The mortality  
 348 rate follows a  $Q_{10}$  relationship, which describes the temperature sensitivity of the  
 349 mortality rate due to increases in temperature by  $10^\circ\text{C}$ . The relationship looks like:

$$350 \quad m(T) = m(20)Q^{\frac{T-20}{10}},$$

351 where  $m(20)$  is the mortality rate at  $20^\circ\text{C}$  and  $Q$  is the factor by which the  
 352 mortality rate increases. A reference temperature of  $20^\circ\text{C}$  is used since that is a  
 353 typical water temperature.

354 The vertical velocity is a function of dynamic viscosity since the higher the vis-  
 355 cosity, the thicker the water, the harder it is for cyanobacteria to float and thus the  
 356 slower they float to the surface. Further, dynamic viscosity varies with temperature,  
 357 the lower the temperature the higher the viscosity. The relationship between vertical  
 358 velocity and temperature is modeled as:

$$359 \quad v(T) = \frac{\eta(20)}{\eta(T)}v(20),$$

360 where  $\eta(T)$  is the dynamic viscosity dependent on temperature, and  $\eta(20)$  and  
 361  $v(20)$  are the dynamic viscosity and vertical velocity at the reference temperature of  
 362  $20^\circ\text{C}$ . Dynamic viscosity is dependent on temperature and this relationship is modeled  
 363 as [3] :

$$364 \quad \eta(T) = \frac{1.78 \times 10^{-3}}{1 + 0.0337T + 0.00022T^2}.$$

365 The term,  $\mu(I, T)C - m(T)C$  describes the net growth or mortality of cyanobac-  
 366 teria in the lake and contributes to whether the population is growing or shrinking.  
 367 If  $\mu > m$ , it is a source term and there is a gain in concentration; if  $\mu < m$ , it is  
 368 a sink term and there is a loss in concentration. The term  $\frac{\partial}{\partial z}(v(T)C)$  describes the  
 369 advection of the population and contributes to how the population is concentrated at  
 370 different depths. Since cyanobacteria have a positive floating velocity this means they  
 371 will advect to the surface of the lake with growth, and the density at a given depth  
 372 can change due to changes in vertical velocity at that depth. The term  $\frac{\partial}{\partial z} \left( D_z \frac{\partial C}{\partial z} \right)$   
 373 describes the diffusion of the population and contributes to the population evenly  
 374 spreading over the depth, which means areas with low density gain more while areas  
 375 with particularly high density lose some of that density.

376 **3.2. Model Analysis.** IBVP (3.1) was analyzed by nondimensionalizing the  
 377 model with,  $\tilde{t} = \frac{D}{L^2}t$  and  $\tilde{z} = \frac{z}{L}$  where  $L$  is the depth of the euphotic layer. Introducing  
 378 this scaling into equation (3.1) yields,

$$(3.2) \quad \begin{cases} \frac{\partial C}{\partial t} = \frac{\partial^2 C}{\partial \tilde{z}^2} + P_e \frac{\partial C}{\partial \tilde{z}} + GC \\ P_e C(0, \tilde{t}) - \frac{\partial C(0, \tilde{t})}{\partial \tilde{z}} = 0 \\ C(1, \tilde{t}) = 0 \\ C(\tilde{z}, 0) = f(\tilde{z}). \end{cases}$$

where the Peclet number,  $P_e = \frac{vL}{D_z}$ , is the ratio of the advection rate to the diffusion rate, the growth Peclet number,  $G = \frac{\mu L^2}{D_z}$ , is the ratio of the growth rate to the diffusion rate. An inequality is derived in Section 3.3 that compares  $P_e$  to  $G$  to indicate whether conditions are conducive for a bloom to occur.

Parameter	Description	Value	Units	Source
<i>Bloom Stability</i>				
$v$	Sinking or flotation velocity	$1.4e^{-4}$	m s <sup>-1</sup>	Jöhnk [6]
$L$	Euphotic layer length	2.81	m	DNR [16]
$P_e$	Peclet number	0-4	—	Simulations
$G$	Growth Peclet number	0-12	—	Simulations
$\lambda$	Degree of freedom	$\pi/2 - \pi$	—	Simulations

The following two subsections report the conclusions from investigating the IBVP (3.2) both analytically and numerically. An analytic solution is used to determine a stability condition signifying when the concentration “blows-up” versus when the concentration collapses. This condition is independent of the initial condition and depends solely on  $P_e$ ,  $G$ , and an eigenvalue that arises from solving the IBVP (3.2). A numerical solution is used for efficient experimentation over a large parameter space and, most importantly, for a variety of initial conditions. Note that an analytic solution is expressed as an infinite Fourier series with coefficients that are expressed as integrals involving the initial condition. The series needs to be truncated and even a rather innocuous initial condition could lead to Fourier coefficients with no closed-form integral. In summary, a numerical solution is inevitable for experimentation so a numerical scheme like the one outlined below is the most efficient means for such exploration and the value of the analytic solution is the stability condition for the concentration.

**3.3. Bloom Stability Condition.** IBVP (3.2) was solved as follows:

1. The transform  $C = e^{-(\frac{P_e}{2})^2 + G}\tilde{t} - \frac{P_e}{2}\tilde{z} u$  was used to reduce equation (3.2) to a simple diffusion IBVP in terms of  $u$ .
2. Separation of variables was used to construct a Fourier series expansion for  $u$  after the boundary conditions were imposed.
3. The initial condition was left in terms of  $f(\tilde{z})$  for generality.
4. The solution,  $u$ , was substituted into the equation for  $C$  in step (1) above.

These steps yield the concentration profile,

$$(3.3) \quad C(\tilde{z}, \tilde{t}) = \sum_{n=0}^{\infty} c_n e^{(-\lambda_n^2 - (\frac{P_e}{2})^2 + G)\tilde{t}} \left( \sin(\lambda_n \tilde{z}) + \frac{2}{3P_e} \lambda_n \cos(\lambda_n \tilde{z}) \right),$$

where the Fourier coefficients  $c_n$  are computed using the integral:

$$c_n = \frac{1}{2} \int_0^1 f(\tilde{z}) e^{(\frac{P_e}{2} - i\lambda_n)\tilde{z}} d\tilde{z}.$$

412 The  $\lambda_n$  are computed by solving the nonlinear eigenvalue problem,

413 (3.4) 
$$\sin(\lambda_n) + \frac{2}{3P_e}\lambda_n \cos(\lambda_n) = 0,$$

414 for a given Peclet number,  $P_e$ .

415 All expressions dependent upon  $\tilde{z}$  are bounded and if the initial condition is  
 416 continuous,  $f(\tilde{z}) \in C([0, 1])$ , as is often the case, then all  $c_n$  converge and are bounded  
 417 as well. The terms dependent upon  $\tilde{t}$  are the main focus of this analysis since they  
 418 have the potential to increase to infinity, which would make the series diverge and  
 419 indicate a bloom has occurred. If the eigenvalues,  $\lambda_n$ , satisfy the condition,

420 (3.5) 
$$-\lambda_n^2 - \left(\frac{P_e}{2}\right)^2 + G < 0,$$

421 then the concentration decays exponentially and the series converges to zero im-  
 422 plying cyanobacteria population collapse, that is, no bloom occurs. Otherwise the  
 423 concentration tends to infinity as  $t$  tends to infinity and the solution diverges imply-  
 424 ing the cyanobacteria population grows without bound, that is, a bloom occurs. Of  
 425 course the cyanobacteria population in this case becomes nutrient limited for the lake  
 426 considered but this case is investigated using a different model in Section 2.

427 The eigenvalues,  $\lambda_n$ , play a prominent role in the stability analysis of equation  
 428 (3.3) so it is important to investigate their behavior. One can use Newton's method  
 429 to solve for  $\lambda_n$  and the formulation given in equation (3.4) is most stable. However,  
 430 it is simpler to study the features of  $\lambda_n$  if equation (3.4) is rewritten as,

431 (3.6) 
$$\tan(\lambda_n) = -\frac{2}{3P_e}\lambda_n.$$

432 The nonlinear equation (3.6) reveals that the eigenvalues,  $\lambda_n$ , have the following  
 433 features for all  $n \geq 0$ , see Figure 8:

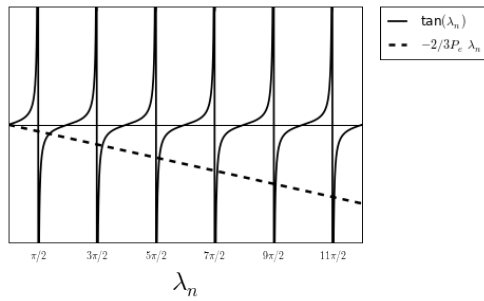


FIG. 8. For varying values of  $\lambda_n$ , the solid lines represent  $\tan(\lambda_n)$  and the dotted line represents  $-\frac{2}{3P_e}\lambda_n$ . Their intersection shows where the eigenvalue condition (3.6) is satisfied.

- 434 • monotonically increasing,  $\lambda_0 < \lambda_1 < \lambda_2 < \dots$   
 435 • if  $P_e \rightarrow \infty$ , then  $\lambda_n \rightarrow n\pi$   
 436 • if  $P_e \rightarrow 0$ , then  $\lambda_n \rightarrow \frac{(2n-1)\pi}{2}$   
 437 •  $\frac{(2n-1)\pi}{2} < \lambda_n < n\pi$

438 •  $\lambda_n \sim \frac{2n-1}{2}\pi + \frac{3P_e}{\pi(2n-1)}$  asymptotically with  $n > P_e$

439 Note that  $\lambda_0 = 0$  yields the trivial solution for the concentration so this case is  
 440 ignored. These features reveal that if the stability condition equation (3.5) fails for  
 441  $\lambda_1$ , it will fail for all remaining eigenvalues. Newton’s method was run on equation  
 442 (3.4) for each  $P_e$  with a tolerance of  $10^{-5}$  in order to determine  $\lambda_1$ . Figure 9 shows  
 443 the range of values and the asymptotic behavior of  $\lambda_1$ , notice that indeed  $\frac{\pi}{2} < \lambda_1 < \pi$ .

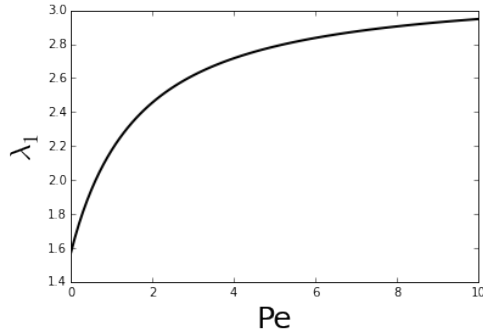


FIG. 9. Given a value for  $P_e$ ,  $\lambda_1$  is determined by using Newton’s method and equation (3.4).

444 Now that the role of  $\lambda_1$  has been established in inequality (3.5) and it is clear  
 445 that Newton’s method can be used to determine its values, a stability condition can  
 446 be written in terms of an upper bound on the growth parameter  $G$ . The stability  
 447 condition for the non-dimensional case is,

448 (3.7) 
$$G < \lambda_1^2 + \frac{P_e^2}{4}.$$

449 This condition reveals the circumstances under which the concentration remains  
 450 bounded and consequently leads to a population collapse. So inequality (3.7) will  
 451 hence be referred to as the “bloom stability condition.” When the bloom stability  
 452 condition (3.7) is satisfied the population collapses and the concentration tends to  
 453 zero otherwise the bloom grows unconditionally and is classified as unstable. The  
 454 bloom stability condition is best summarized using the plot in Figure 10. Notice that  
 455 it divides the first quadrant into two regions, one for population collapse and one for  
 456 population growth.

457 If the cyanobacteria are in a nutrient-limited environment, then their growth  
 458 depends on phosphorus uptake. Under these circumstances concentration collapse or  
 459 growth hinges on the magnitude of the turbulent diffusivity,  $D_z$ . Rewriting inequality  
 460 (3.7) in dimensional terms yields an upper bound on the turbulent diffusivity,  $D_z$ ,

461 
$$0 < \left(\frac{\lambda_1}{L}\right)^2 D_z^2 - \mu D_z + \left(\frac{v}{2}\right)^2.$$

462 If the advective velocity,  $v$ , and the euphotic layer,  $L$ , are held fixed, then Fig-  
 463 ure 11 shows that that there is a condition under which the concentration will grow or  
 464 collapse. Expressed in dimensional terms, the condition under which the population  
 465 will collapse is now,

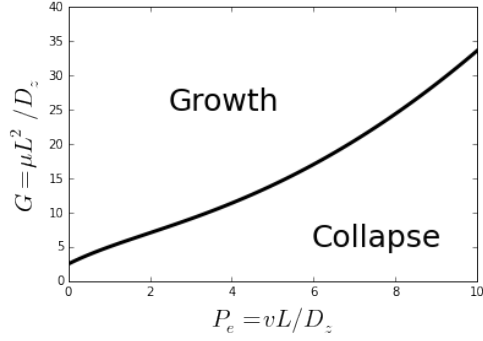


FIG. 10. The bloom stability condition separates the quadrant into two regions, if  $G < \lambda_1^2 + \frac{P_c^2}{4}$ , then the population experiences collapse, otherwise the population experiences unbounded growth.

466 (3.8) 
$$D_z > \frac{\mu}{2} \left( \frac{L}{\lambda_1} \right)^2 \left[ 1 + \sqrt{1 - \left( \frac{\lambda_1 v}{\mu L} \right)^2} \right].$$

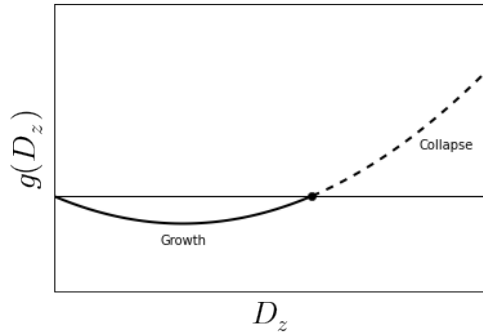


FIG. 11. The bloom stability condition in dimensional terms. In a nutrient-limited environment, the bound on the turbulent diffusivity,  $D_z$ , establishes the limitation on growth.

467 Given that  $\frac{\pi}{2} < \lambda_1 < \pi$  and suppose that  $\left( \frac{\lambda_1 v}{\mu L} \right)^2 \ll 1$ , then inequality (3.8)  
 468 simplifies to a similar criterion provided in [19],

469 (3.9) 
$$D_z > \frac{4\mu L^2}{\pi^2}.$$

470 Moreover, inequality (3.8), establishes a minimum criteria for the growth param-  
 471 eter,  $\mu$ . If the expression under the radical is to remain real, then

472 (3.10) 
$$\mu > \frac{\lambda_1 v}{L},$$

473 to maintain concentration growth. This requirement implies a nutrient limitation and  
 474 the existence of a carrying-capacity for the cyanobacteria population. A modified

475 model based on the one given in [13] is given in Section 2 where a carrying-capacity  
 476 is included to forecast the concentration levels in the lake in a nutrient-limited envi-  
 477 ronment. Again, since  $\frac{\pi}{2} < \lambda_1 < \pi$ , inequality (3.10) is bounded below and can be  
 478 written,

$$479 \quad (3.11) \quad \mu > \frac{\pi v}{2L}.$$

480 Combining inequalities (3.9) and (3.11) yields a simpler stability criterion in a  
 481 nutrient-limited environment where the growth parameter is suitably large enough to  
 482 support growth. Again, if  $\left(\frac{\lambda_1 v}{\mu L}\right)^2 \ll 1$  then the inequality is completely dependent  
 483 upon the sinking velocity and the euphotic layer,

$$484 \quad (3.12) \quad D_z > \frac{2}{\pi} v L.$$

485 If the turbulent diffusivity satisfies this criterion, then the population collapses,  
 486 otherwise it grows. Inequality (3.12) may be used in the event that one assumes the  
 487 growth parameter is high enough to support growth and is searching for a turbulent  
 488 diffusivity that can bring about population collapse in this “worst-case scenario.”  
 489 Otherwise, one can look to bring about collapse by limiting  $\mu$  and increasing  $D_z$ .

490 Currently there is not data available to verify this model. However there are plans  
 491 for a real time sensor that can collect chlorophyll-a concentration and turbulence of  
 492 the water. Once this data is collected this model can be verified.

493 **4. Conclusion.** A logistic model (2.1) was proposed to forecast the chlorophyll-a  
 494 concentration in Tainter Lake. This model was shown to have a steady-state solution  
 495 (2.2), that is a function of the growth rate, thus indicating that the *M. aeruginosa*  
 496 population is time and resource dependent. After a flushing event occurs there is  
 497 lag before the population grows and the chlorophyll-a increases to the steady-state.  
 498 One can use the model to test a variety of parameters for the growth rate to forecast  
 499 concentration levels over time.

500 A second model (3.1) was proposed for analysis to better understand both the  
 501 biologic and limnologic conditions that cause algae blooms. This model was used to  
 502 arrive at a bloom-stability condition solely dependent upon the sinking velocity and  
 503 the euphotic layer, (3.12). One can use the model to test if a combination parameters  
 504 will bring about population collapse.

505 These models may be used in tandem to make predictions involving proposed  
 506 solutions to mitigate the algal blooms in Lake Tainter. Both models suggest lowering  
 507 the growth rate of algae can prevent the population from growing too large. The  
 508 growth rate can be lowered by limiting the amount of nutrients that are allowed  
 509 into the lake. Model (3.1) suggests increasing turbulence can bring about population  
 510 collapse. This can be done by undamming the lake or by installing lake bubblers that  
 511 manually aerate and disturb the lake.

512 **Acknowledgments.** The authors would like to acknowledge the assistance of  
 513 Stephen Nold and William James for their invaluable guidance in the writing of this  
 514 manuscript.



FORECASTING ALGAL BLOOM LAGS AND STABILITY

- 516 [1] M. BOYLE AND K. KIEL, *A survey of house price hedonic studies of the impact of environmental*  
517 *externalities*, Journal of Real Estate Literature, 9 (2001), pp. 117–144, [http://aresjournals.](http://aresjournals.org/doi/abs/10.5555/reli.9.2.23u082061q53qpm3?code=ares-site)  
518 [org/doi/abs/10.5555/reli.9.2.23u082061q53qpm3?code=ares-site](http://aresjournals.org/doi/abs/10.5555/reli.9.2.23u082061q53qpm3?code=ares-site) (accessed 2018/01/10).
- 519 [2] W. DODDS, *Freshwater Ecology: Concepts and Environmental Applications*, Academic Press,  
520 San Diego, C.A., 2002.
- 521 [3] K. HUTTER AND K. JOHNK, *Continuum Methods of Physical Modeling - Continuum Mechanics,*  
522 *Dimensional Analysis, Turbulence*, Springer, Berlin, G.R., 2004.
- 523 [4] W. JAMES, S. NOLD, L. ANDERSON, , R. FLECK, H. LIEFFORT, N. LOEVEN, L. PROVOS,  
524 M. VANDENBERG, AND A. WILSON, *Limnological conditions in tainter and menomin reser-*  
525 *voirs: Interim report 2017*. Discovery Center - Sustainability Research and Rehabilitation,  
526 Menomonie, WI 54751, 2017.
- 527 [5] A. JANSSEN AND S. T. ET AL, *Alternative stable states in large shallow lakes?*, Journal of Great  
528 Lakes Research, 40 (2014), pp. 813–826, <https://doi.org/10.1016/j.jglr.2014.09.019>.
- 529 [6] K. JOHNK AND J. H. ET AL, *Summer heatwaves promote blooms of harmful cyanobacteria,*  
530 *Global Change Biology*, 14 (2008), pp. 495–512, [https://doi.org/10.1111/j.1365-2486.2007.](https://doi.org/10.1111/j.1365-2486.2007.01510.x)  
531 [01510.x](https://doi.org/10.1111/j.1365-2486.2007.01510.x).
- 532 [7] J. KRONKAMP, A. V. D. HEUVEL, AND L. MUR, *Phosphorus uptake and photosynthesis by*  
533 *phosphate-limited cultures of the cyanobacterium microcystis aeruginosa*, British Phycolog-  
534 ical Society, 24 (1989), pp. 347–355, <https://doi.org/10.1080/00071618900650361>.
- 535 [8] C. KRYSSEL, E. M. BOYER, C. PARSON, AND P. WELLE, *Lakeshore property values and water*  
536 *quality: Evidence from property sales in the mississippi headwaters region*. Legislative  
537 Commission on Minnesota Resources by the Mississippi Headwaters Board and Bemidji  
538 State University, 2003.
- 539 [9] H. PAERL, R. FULTON, P. MOISANDER, AND J. DYBLE, *Harmful freshwater algal blooms with*  
540 *an emphasis on cyanobacteria*, The Scientific World, 1 (2001), pp. 76–113, [https://doi.](https://doi.org/10.1100/tsw.2001.16)  
541 [org/10.1100/tsw.2001.16](https://doi.org/10.1100/tsw.2001.16).
- 542 [10] H. PAERL AND T. OTTEN, *Harmful cyanobacterial blooms: Cause, consequences, and controls,*  
543 *Microbial Ecology*, 65 (2013), pp. 995–1010, <https://doi.org/10.1007/s00248-012-0159-y>.
- 544 [11] H. PEDROTTI, C. DELANEY, E. MELLY, AND D. FERGUSON, *Economic impacts of algae: An*  
545 *hedonic pricing analysis of water quality valuation*. Working paper, 2017.
- 546 [12] SCI.PY.ORG, *scipy.integrate.odeint*, 2004, [http://docs.scipy.org/doc/scipy/reference/generated/](http://docs.scipy.org/doc/scipy/reference/generated/scipy.integrate.odeint.html)  
547 [scipy.integrate.odeint.html](http://docs.scipy.org/doc/scipy/reference/generated/scipy.integrate.odeint.html) (accessed 2016/07/29).
- 548 [13] D. SOBALLE AND S. THRELKELD, *Advection phytoplankton biomass and nutrient transforma-*  
549 *tions in a rapidly flushed impoundment*, Archiv fur Hydrobiologie, 105 (1985), pp. 187–203.
- 550 [14] UNITED STATES GEOGRAPHICAL SURVEY, *Usgs 05367500 red cedar river near colfax, wi*, 2015,  
551 [http://nwis.waterdata.usgs.gov/usa/nwis/uv/?cb\\_00060=on&cb\\_00065=on&format=](http://nwis.waterdata.usgs.gov/usa/nwis/uv/?cb_00060=on&cb_00065=on&format=html&site_no=05367500&period=&begin_date=2015-05-01&end_date=2015-10-10)  
552 [html&site\\_no=05367500&period=&begin\\_date=2015-05-01&end\\_date=2015-10-10](http://nwis.waterdata.usgs.gov/usa/nwis/uv/?cb_00060=on&cb_00065=on&format=html&site_no=05367500&period=&begin_date=2015-05-01&end_date=2015-10-10) (ac-  
553 cessed 2016/07/29).
- 554 [15] WEATHER UNDERGROUND, *Weather history for colfax, wi*, 2015, [https://www.wunderground.](https://www.wunderground.com/personal-weather-station/dashboard?ID=KWICOLFA3&scrollTo=historyTable#history/s20150501/e20150501/mdaily1)  
555 [com/personal-weather-station/dashboard?ID=KWICOLFA3&scrollTo=historyTable#](https://www.wunderground.com/personal-weather-station/dashboard?ID=KWICOLFA3&scrollTo=historyTable#history/s20150501/e20150501/mdaily1)  
556 [history/s20150501/e20150501/mdaily1](https://www.wunderground.com/personal-weather-station/dashboard?ID=KWICOLFA3&scrollTo=historyTable#history/s20150501/e20150501/mdaily1) (accessed 2016/07/29).
- 557 [16] WISCONSIN DEPARTMENT OF NATURAL RESOURCES, *Phosphorus Total Maximum Daily Loads,*  
558 2012.
- 559 [17] WISCONSIN DEPARTMENT OF NATURAL RESOURCES, *Lake water quality 2015 annual re-*  
560 *port: Tainter lake middle basin*, 2015, [https://dnrx.wisconsin.gov/swims/public/](https://dnrx.wisconsin.gov/swims/public/reporting.do?type=10&action=post&stationNo=173215&year1=2015&format=html)  
561 [reporting.do?type=10&action=post&stationNo=173215&year1=2015&format=html](https://dnrx.wisconsin.gov/swims/public/reporting.do?type=10&action=post&stationNo=173215&year1=2015&format=html) (ac-  
562 cessed 2016/07/29).
- 563 [18] WISCONSIN DEPARTMENT OF NATURAL RESOURCES, *Tainter lake*, 2015, [http://dnr.wi.gov/](http://dnr.wi.gov/lakes/lakepages/LakeDetail.aspx?wbic=2068000&page=facts)  
564 [lakes/lakepages/LakeDetail.aspx?wbic=2068000&page=facts](http://dnr.wi.gov/lakes/lakepages/LakeDetail.aspx?wbic=2068000&page=facts) (accessed 2016/07/29).
- 565 [19] K. WONG, J. LEE, AND I. HODGKISS, *A simple model for forecast of coastal algal blooms,*  
566 *Estuarine, Coastal, and Shelf Science*, 74 (2007), pp. 175–196, [https://doi.org/10.1016/j.](https://doi.org/10.1016/j.ecss.2007.04.012)  
567 [ecss.2007.04.012](https://doi.org/10.1016/j.ecss.2007.04.012).